Efficient hybrid polymer/TiO_2 solar cells using a multilayer structure

P. Ravirajan[*, 1, 2], A. Green[3], S. A. Haque[3], J. R. Durrant[3], D. D. C. Bradley[1] and J. Nelson[1]

[1]Centre for Electronic Materials and Devices, Dept. of Physics, Imperial College London, Prince Consort Road, London SW7 2BW, U.K;

[2]Dept. of Physics, University of Jaffna, Jaffna, Sri Lanka;

[3]Centre for Electronic Materials and Devices, Dept. of Chemistry, Imperial College London, Exhibition Road, London SW7 2AZ, U.K

ABSTRACT

This study focuses on systems consisting of high hole-mobility MEHPPV based polymers or a fluorene-bithiophene co-polymer in contact with different nanocrystalline TiO_2 films. We use photoluminescence quenching, time of flight mobility measurements and optical spectroscopy to characterize the exciton transport, charge transport and light harvesting properties, respectively, of the polymers, and correlate these material properties with photovoltaic device performance. We find that the polymer properties with greatest influence on device efficiency are the polymer exciton diffusion length and absorption range, followed by the hole mobility. We have also studied the photovoltaic performance of these TiO_2/polymer devices as a function of active layer thickness. Device performances are significantly improved by introducing a PEDOT layer between the polymer and the top Au electrode and by reducing the thickness of the active layers. The optimized devices have peak external quantum efficiencies $\approx$ 40 % at the polymer's maximum absorption wavelength and yield short circuit current densities $\geq$ 2 mA cm^{-2} for air mass (AM) 1.5 conditions (100 mW cm^{-2}, 1 sun). The AM 1.5 open circuit voltage reaches 0.64 V and the fill factor 0.43, resulting in an overall power conversion efficiency of 0.58 %.

Keywords: Solar cells, Polymer, Nanocrystalline TiO_2, polymer, PEDOT, exciton diffusion length, hole mobility

1. INTRODUCTION

Polymer/fullerene solar cells are the best studied polymer based solar cells and to date have yielded the highest efficiencies[1]. However, the use of fullerenes as electron acceptors has some disadvantages, such as segregation of the components during ageing and relatively poor photo stability. Hybrid polymer/metal oxide solar cells are a promising class of polymer based solar cells due to the attractive properties of the metal oxide such as stability, electron transport properties, and the possibilities for controlling surface morphology. In addition, metal oxides offer ease of fabrication and low cost. Since the first observation of efficient photoinduced charge separation in a TiO_2/MEH-PPV polymer composite[2], there have been many studies in TiO_2 with several other conjugated polymers[3-5]. Despite the effective combination of polymer and TiO_2, the highest external quantum efficiency, EQE (25 % at 435 nm[5]) and power conversion efficiencies (< 0.2 % under 1 sun[6]) reported previously are still low compared to the best values for other polymer-based solar cells. Performance is typically limited by the low EQE, which leads to low AM 1.5 short circuit current densities, J_{SC}[2-7] of only a few hundreds of μA cm^{-2} compared to over 5 mA cm^{-2} for polymer-fullerene devices made from similar polymers. The reduced J_{SC} may be due to a number of factors: limited red absorbance, small optical depth, poor sensitization of the oxide film, thicker active layer thickness, large pore size / nanostructure scale compared to the exciton diffusion length, poor charge transport, fast recombination, or imperfect interfaces. However, it is difficult to analyze these losses on the basis of previous studies, on account of wide variations in materials and fabrication techniques. In this paper, we attempt to identify the mechanisms limiting the short circuit current density, through a systematic study of the effect of the optoelectronic properties of the polymer and active layer thickness on the performance of the polymer-TiO_2 hybrid system.

[*]p_ravirajan@jfn.ac.lk

Organic Photovoltaics V, edited by Zakya H. Kafafi, Paul A. Lane,
Proceedings of SPIE Vol. 5520 (SPIE, Bellingham, WA, 2004)
0277-786X/04/$15 · doi: 10.1117/12.561212

2. EXPERIMENTAL

2.1 Materials

Three MEH-PPV based and one fluorene-bithiophene hole-transporting polymers have been used in this work and their chemical names and structures[8,9] are shown in Figure 1 (a), (b), (c) and (d). The first two MEH-PPV polymers contain TPD groups. The TPD (4M)-MEH-M3EH-PPV polymer is a statistical polymer, while the others are alternating copolymers.

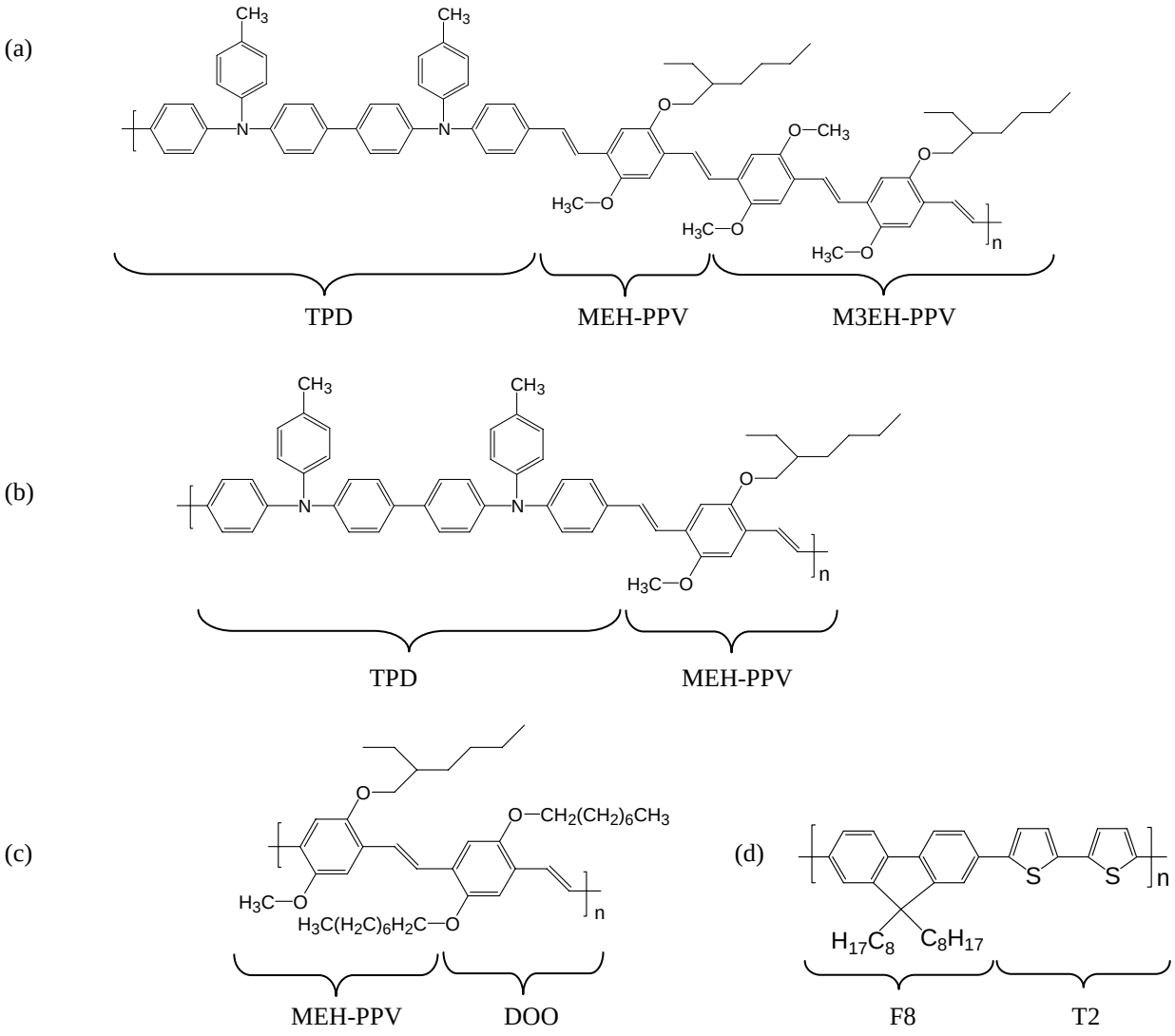

Figure 1 Chemical structures[8,9] of (a) Poly[(1,4-phenylene-(4-methyl phenyl)amino-4,4'-diphenylene-(4-methylphenyl)amino-1,4-phenylene-ethenylene-2-methoxy-5-(2-ethylexyloxy)-1,4-phenylene-ethenylene)-co-(2,5-dimethoxy-1,4-phenylene-ethenylene-2-methoxy-5-(2-ethylhexyloxy)-1,4-phenylene-ethenylene)] TPD(4M)-MEH-M3EH-PPV terpolymer (b) Poly[(4-methylphenyl) amino-4,4'-diphenylene-(4-methylphenyl)amino-1,4-phenylene-ethenylene-2-methoxy-5-(2-ethylhexyloxy)-1,4-phenylene-ethenylene-1,4-phenylene] TPD(4M)-MEH-PPV copolymer (c) Poly[2-methoxy-5-(2-ethylhexyloxy)-1,4-phenylene-ethenylene-2,5-dioctyloxy-1,4-phenylene-ethenylene] MEH-DOO-PPV copolymer (d) Poly(9,9-dioctylfluorene-co-bithiophene) (F8T2) copolymer.

Two different TiO_2 pastes, which we will refer to as aqueous and organic, having different size of TiO_2 colloidals, were used in this study. The aqueous paste contained colloids of about 15 nm diameter and was synthesised as described in Ref.[10] at Imperial College London, while organic paste contained 20 nm diameter colloids dispersed in an organic mixture (terpineol/ethylcellulose)[11] was received from the Energy Centre for Netherlands.

2.2 Sample fabrication

Samples were prepared on Indium Tin Oxide (ITO) coated glass substrates, Fluorine doped Tin Oxide (FTO) coated glass substrate or spectrosil B substrate which were first cleaned by ultrasonic agitation in acetone and isopropanol. For cyclic voltammetry and optical absorption measurements, polymer samples were prepared by spin coating on FTO substrate and spectrosil respectively. Single layer (polymer) and bi-layer (polymer and dense TiO_2) samples with different layer thicknesses were prepared on ITO for exciton diffusion length measurements. Samples for time-of-flight measurements were also prepared on ITO and the top contact was Aluminium (~50 nm). The thickness of the polymer film for TOF measurement was typically between 1 and 1.5 μm.

For devices, four layers were prepared on top of the ITO substrate, namely a dense TiO_2 'Hole Blocking' layer (HBL), a porous nanocrystalline TiO_2 layer, a dip-coated polymer layer and a spin-coated polymer layer as well as a metal top contact. The porous TiO_2 layer is required to increase the interfacial area for charge separation, as shown in Ref [4]. The dip coating step improves both the sensitisation of the TiO_2 film compared to spin coating alone and the fill factor of the TiO_2/polymer device leading to an overall power conversion efficiency by 50 %[12]. The final, spin coated polymer layer is required to fill the pores, thus increasing optical density and improving film uniformity[4,12]. In some devices, a PEDOT layer was deposited on top of the polymer layer before depositing the metal contact. The ITO substrate was first covered with a thin dense TiO_2 layer using a spray pyrolysis technique[13]. The porous TiO_2 layer was deposited by spin coating the diluted aqueous TiO_2 paste or organic TiO_2 paste (dissolved in tetrahydrofuran) on to the dense TiO_2 layer. The spin coated porous TiO_2 layers were then sintered at 450 ^{0}C for 30 minutes in air. The dip-coated layer was prepared on the porous TiO_2 layer by immersing the TiO_2 electrode in a solution of polymer in C_6H_5Cl (~2 mg/ml) at 50-60 ^{0}C overnight. The dip-coated film was then "wiped" by a quick blow with dry nitrogen gas (oxygen free) and heated at about 50 ^{0}C in air. A 50 nm polymer layer was then deposited on the substrate by spin coating from a polymer solution in C_6H_5Cl (10 mg/ml) at 2000 rpm. The thickness of each of the films on both ITO and spectrosil was measured by a Tencor Alpha-Step 200 profilometer, while the effective polymer thickness on porous TiO_2 was estimated by comparing the optical absorption of the polymer coated TiO_2 electrode with the known absorption coefficient of the polymer on spectrosil, assuming that the TiO_2 is ~ 50% porous. The deposition of PEDOT on top of the polymer is somewhat tricky as we normally observe less adherence of PEDOT with polymer if we do not adopt the following procedures: The PEDOT (PEDOT:PSS) solution is first ultrasonicated for 10 minutes and then heated for 5 minutes at 90 ^{0}C. The solution is then filtered with a 0.45 μm filter and spin-coated on the dried semiconducting polymer layer in a water free environment. The sample is then annealed at 100 ^{0}C for 5 minutes in a glove box which was filled with dry N_2 gas. Au electrodes are deposited either onto the polymer film or the PEDOT film by thermal evaporation though a shadow mask. The Au contacted devices are annealed again at 100 ^{0}C for 5 minutes in a N_2 gas environment. It is essential that the PEDOT layer should be annealed for not more than 15 minutes because a longer annealing time degrades the layer[14]. There were six devices per substrate to check reproducibility and the area each active device was about 4.2 mm^2. The thicknesses of the layers was as follows unless stated otherwise: HBL (~40 nm) / porous TiO_2 (~100 nm) / polymer (~50 nm) / PEDOT (~50 nm) / Au (~60 nm).

2.3 Sample characterisation

Time-of-flight measurements were made using a Nd:YAG frequency-tripled laser (λ = 355 nm, τ = 6 ns, 2 Hz) as the excitation source. The sample was illuminated from the ITO side. Care was taken to keep the generated charge less than 5 % of the capacitor charge stored on the sample to avoid space-charge effects. For exciton diffusion length measurements, the relative photoluminescence (PL) intensity at wavelength corresponds to about peak PL intensity was measured as a function of polymer thickness spin coated on ITO substrates and with an additional 50 nm dense TiO_2 layer using a FluoroMax 3.0 spectrofluorimeter with 440 nm excitation through the substrate. Cyclic voltammetry (CV) measurements were also carried out to determine the ionization potential of all four polymers using a standard three electrode cell comprising a Pt wire as counter electrode, the polymer film on F doped SnO_2 as the working electrode and an Ag/AgCl reference electrode. A redox inactive electrolyte (0.1 M tetrabutylammonium tetrafluoroborate) was used to minimize the effect of transport of analyte through migration to the working electrode. The electrolyte solution was prepared in a glove box filled with dry nitrogen gas. The J-V measurements were taken in air under simulated sunlight using a home built computer controlled potentiostat measurement unit and a halogen lamp calibrated to an air mass (AM) 1.5. For EQE measurements, the photocurrent of the sample, and the photocurrent of a calibrated silicon photodiode were obtained at a particular position for different wavelengths. The intensity of the light was calculated as a function of wavelength using the known spectral response and measured photocurrent spectrum of the silicon photodiode held at the same position as the sample.

3. RESULTS

3.1 Optoelectronic properties of the polymers

3.1.1 Optical absorption of the polymers

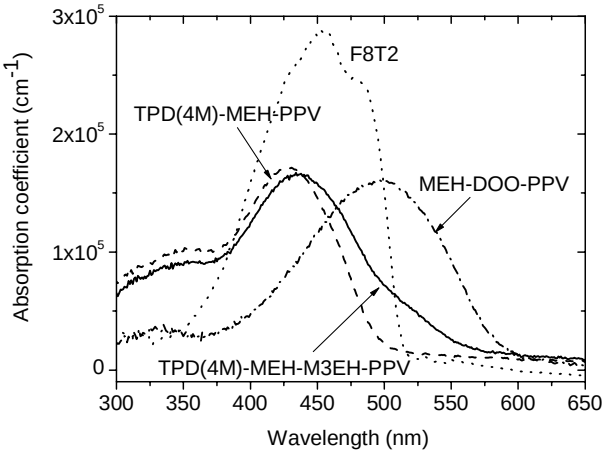

Figure 2 UV-VIS optical absorption spectra for polymer films on spectrosil B substrates.

Optical absorption spectra for thin films of each of the three MEH-PPV polymers and the fluorene-bithiophene polymer spin-coated on spectrosil B substrates are shown in Figure 2. The magnitude of the absorption coefficient is similar for all MEH-PPV based polymers, while F8T2 polymer has higher absorption coefficient than any of these MEH-PPV polymers in the wavelength range from 375 nm to 500 nm. F8T2 has a broad optical absorption in the visible spectrum peaking at about 460 nm, while MEH-DOO-PPV polymer absorbs further into the red, with peak absorption at 502 nm. The absorption spectrum of the TPD (4M) MEH-M3EH-PPV polymer is red shifted slightly compared to that of TPD (4M) MEH-PPV. Whilst TPD (4M) MEH-PPV and MEH-DOO-PPV are strictly alternating copolymers [8,9], the TPD (4M) MEH-M3EH-PPV polymer is a statistical condensation copolymer consisting of TPD (4M) MEH-PPV $(AB)_x$ repeat units and M3EH-PPV $(CB)_y$ repeat units in the ratio x:y = 50:50[9]. The M3EH-PPV units are therefore believed to be responsible for the red shoulder in the absorption of TPD (4M) MEH-M3EH-PPV.

3.1.2 Ionisation potential of the polymers

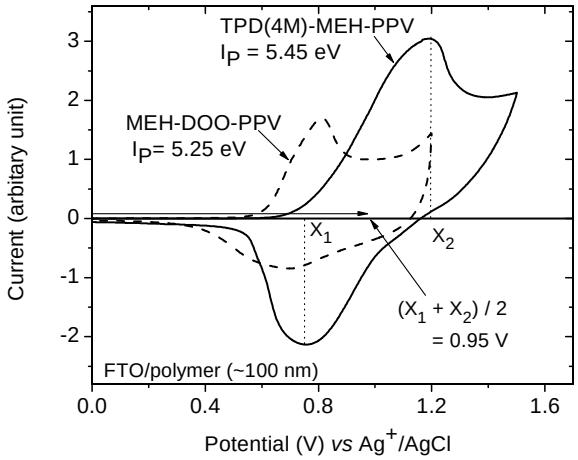

Figure 3 Cyclic voltammograms of spin coated MEH-DOO-PPV (dash line) and TPD (4M)-MEH-PPV (solid line) polymer films on FTO substrates.

Figure 3 shows the cyclic voltammograms of MEH-DOO-PPV and TPD (4M)-MEH-PPV polymer films on F doped SnO_2 substrate (FTO). The oxidation potential of the MEH-DOO-PPV is lower than the TPD (4M)-MEH-PPV polymer. The ionisation potential lies between 5.25 eV and 5.55 eV for all four polymers. The values are compared in the third column of the table I.

3.1.3 Hole mobility of the polymers

The polymer hole-mobilities were studied by the time-of-flight (TOF) method. Figure 4 (a) shows a typical room temperature hole transient for the TPD (4M)-MEH-PPV polymer, in an ITO / polymer (1.2 μm) / Al device structure, at two different electric fields. The inset of Figure 4 (a) shows the corresponding transients on a double logarithmic scale. The transient shows an initial spike followed by a distinctive plateau and then by a broad tail. The constant current plateau in the hole-transient of TPD (4M)-MEH-PPV polymer indicates non-dispersive transport. Figures 4 (b) and (c) show typical hole transients for MEH-DOO-PPV and TPD (4M)-MEH-M3EH-PPV polymers, in ITO / polymer / Al device structures with polymer thicknesses of 1.5 and 1.2 μm respectively. The transients are more dispersive, but still show clear transit times. The comparison of Figures 4 (b) and (c) shows that hole-transport in MEH-DOO-PPV polymer is less dispersive than in TPD (4M)-MEH-M3EH-PPV polymer.

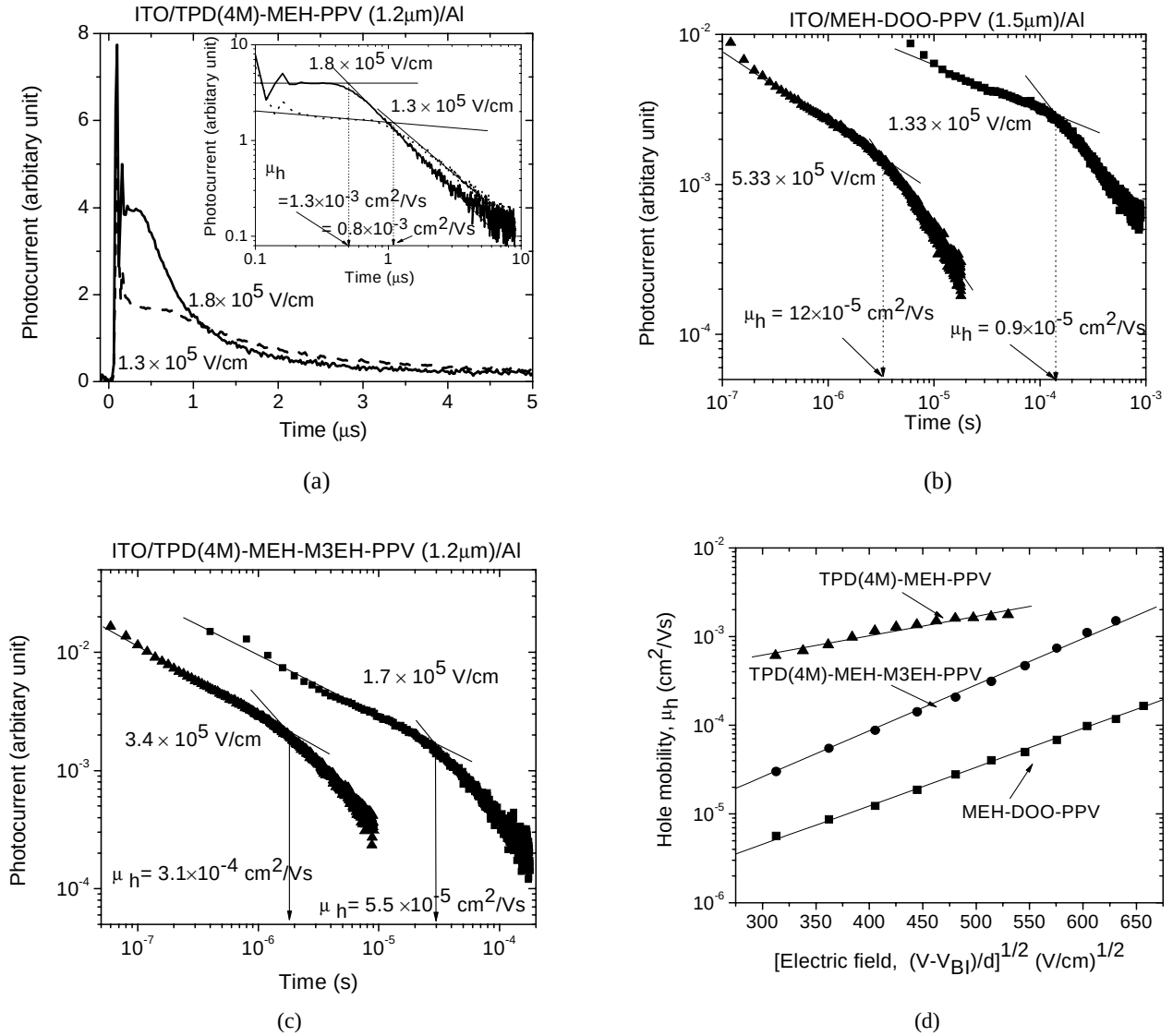

Figure 4 Typical TOF hole transients in (a) ITO / TPD (4M)-MEH-PPV (1.2μm) / Al (b) ITO / MEH-DOO-PPV (1.5μm) / Al, (c) ITO / TPD (4M)-MEH-M3EH-PPV (1.2 μm) / Al device structures at two different fields. (d) The variation of the room temperature TOF hole-mobility μ_h with electric field for these three MEH-PPV based polymers. The built in voltage for the ITO / polymer / Al structure is assumed to be 0.3 V.

The mobility at an applied electric field E was calculated from the expression $\mu = d/(t_T E)$, where d is the polymer thickness and t_T is the transit time. Here, we note that the collected charge was less than 5 % of the sample capacitor charge in all cases. The electric field across the samples can therefore be assumed constant and we can apply this equation in confidence to calculate the mobility of the polymers. The electric field was calculated taking into account a built-in voltage of 0.3 V, namely the workfunction difference between the ITO (4.6 eV) and Al (4.3 eV) electrodes. The work function values of ITO and Al were estimated by Kelvin probe and electroabsorption measurements respectively[4].

Figure 4 (d) shows the electric field dependent variation of the room-temperature hole-mobility for all three MEH-PPV polymers. The hole mobilities of all polymers follow a Poole-Frenkel dependence $\mu_h \propto \exp(\beta E^{1/2})$. The two TPD containing polymers show higher hole-mobility than the MEH-DOO-PPV polymer. This may be due to the positive influence of the TPD group on hole-transport. The TPD (4M)-MEH-PPV polymer shows higher hole mobility than the other two polymers in the range of electric fields from 0.9×10^5 V/cm to 5×10^5 V/cm. The TPD (4M)-MEH-PPV polymer also shows weaker field dependence, while both TPD (4M)-MEH-M3EH-PPV and MEH-DOO-PPV polymers show strong field dependence. Estimating an electric field of 1×10^5 V/cm within an efficient TiO_2/polymer photovoltaic device (polymer thickness ~ 50-100 nm) at short circuit, the TPD (4M)-MEH-PPV polymer would be expected to give the best hole transport in devices. However, hole-transport in both TPD (4M)-MEH-M3EH-PPV and MEH-DOO-PPV polymers should improve in thinner devices. F8T2 polymer shows highly dispersive hole-transport and strongly field dependent TOF hole-mobility in the range of 10^{-5} - 10^{-4} cm^2/Vs over the electric field range 1×10^4 – 6×10^4 V/cm[15] . However, it performs rather better as an aligned thin film in field effect transistor structures and FET hole mobility of F8T2 polymer is 0.01 - 0.02 cm^2/Vs in aligned F8T2 polymer[16], but such alignment cannot be achieved in the present devices.

3.1.4 Exciton diffusion length of the polymers

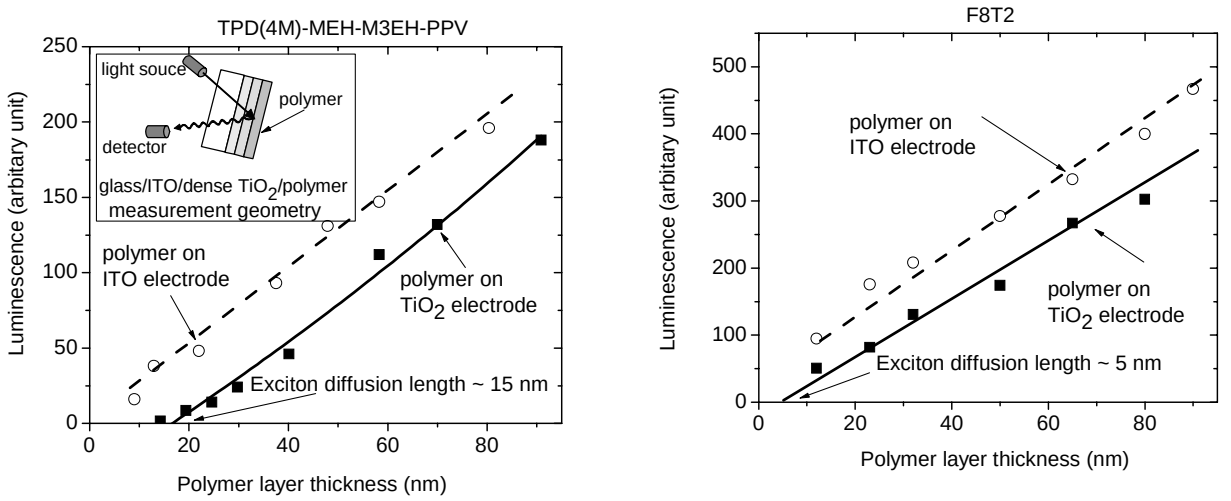

Figure 5 Photoluminescence at 600 nm from a spin-coated polymer layer [(a) TPD (4M)-MEH-M3EH-PPV and (b) F8T2] on ITO (circles) and on ITO / dense TiO_2 (squares) substrates, as a function of polymer layer thickness. The polymers were excited with 400 nm light through the ITO. The inset shows the measurement geometry in the spectrofluorimeter.

The exciton diffusion length in TPD (4M)-MEH-M3EH-PPV and F8T2 polymer was estimated using the method described in Ref. [2]. Figure 5 (a) shows the relative photoluminescence of the TPD (4M)-MEH-M3EH-PPV polymer layers on ITO and dense TiO_2 substrates at 600 nm, as a function of polymer layer thickness when the polymer was excited with 400 nm light through the ITO coated glass substrate. The photoluminescence measurements were taken using a FlouroMax 3.0 spectrofluorimeter and the inset of Figure 5 (a) shows the measurement geometry. The polymer layer thickness on the dense TiO_2 layer was estimated from the UV-VIS optical absorption of the layer using the known absorption coefficient of the polymer. The luminescence varies linearly with polymer layer thickness on ITO, and approximately linearly with polymer thickness on dense TiO_2. For the dense TiO_2 substrate, the trend

predicts complete quenching of luminescence at a layer thickness of about 15 nm, and we can therefore estimate the exciton diffusion length in the polymer as (15 ± 4) nm. This is similar to that determined in MEH-PPV (20 nm) by a similar technique[2]. The other two PPV polymers also contain MEH-PPV sub-units and we may expect that their exciton diffusion lengths would be similar to those of TPD (4M)-MEH-M3EH-PPV and MEH-PPV. We could therefore reasonably assume the exciton diffusion length of MEH-DOO-PPV and TPD (4M)-MEH-PPV polymers are ~15 nm.

Figure 5 (b) shows the relative photoluminescence of the F8T2 polymer layers on ITO and dense TiO_2 substrates at 600 nm, as a function of polymer layer thickness when the polymer was excited with 450 nm light through the ITO coated glass substrate. The luminescence varies linearly with polymer layer thickness on ITO, and on dense TiO_2. For the dense TiO_2 substrate, the trend predicts complete quenching of luminescence at a layer thickness of 5 nm, and we can therefore assume the exciton diffusion length in the polymer as about 5 nm. This value is in good agreement with exciton diffusion length of other polythiophene polymers. Note that exciton diffusion lengths are expected to be shorter in thiophene polymers than in PPV polymer, because of faster singlet-triplet intersystem crossing.

Table I compares the ionisation potential, exciton diffusion length, hole-transport, and absorption properties of these three MEH-PPV polymers and the F8T2 polymer. The ionization potential of each polymer lies between 5.20 eV and 5.55 eV. The last two columns of Table I compare the hole-mobility at a given electric field and the nature of hole transport. The hole mobility of the TPD (4M)-MEH-PPV polymer is higher than the other polymer studied here. However, the spectral absorbance properties are better in MEH-DOO-PPV polymer. Overall, the TPD (4M)-MEH-M3EH-PPV polymer shows the most promising combination of hole-transport and absorption properties for solar cell application.

Table I Summary of optoelectronic parameters for the polymers studied. Where λ_{max} is the wavelength corresponding to maximum absorption, α the corresponding absorption coefficient, I_P the ionization potential, L_d the exciton diffusion length and μ_h the hole mobility, at a fixed electric field.

Polymers	**α ($\times 10^{-5}$cm^{-1})**	**λ_{max} (nm)**	**I_P (eV)**	**L_d (nm)**	**μ_h (cm^2/Vs) at 2.5×10^5 V/cm**	**Type of transport**
MEH-DOO-PPV	1.60	502	5.25	15	3.3×10^{-5}	Dispersive
TPD (4M)-MEH-M3EH-PPV	1.67	439	5.30	15	2.8×10^{-4}	Dispersive
TPD (4M)-MEH-M3EH-PPV	1.74	428	5.45	15	2.0×10^{-3}	Non-dispersive
F8T2	3.10	460	5.55	05	10^{-4} -10^{-5} [15]	Highly dispersive

3.2 Effect of polymer optoelectronic properties on device performance

We now consider the influence of the exciton diffusion length, hole transport and light havesting properties of the polymer on the performance of TiO_2 / polymer phtovoltaic devices. The short circuit current density of a TiO_2/polymer photovoltaic device may depend upon the polymer through its light harvesting properties and exciton diffusion length as well as the uptake of the polymer by porous TiO_2 during dip-coating and spin coating. Good uptake of polymer by the porous TiO_2 is essential for efficient device performance. We found[17] that all of these PPV polymers sensitise the TiO_2 well. We find that F8T2 polymer showed similar polymer uptake by the porous TiO_2 films. Good uptake of MEH-PPV based polymer may be aided by an interaction between the TiO_2 surface and the oxygen atoms of the alkoxy substituents on the MEH-PPV subunits of each polymer. The TPD (4M)-MEH-M3EH-PPV polymer shows better uptake by TiO_2 than the other two PPV polymers. This may be due to the higher number of alkoxy substituents in the polymer repeat unit (see Figure 1). Another reason for the better sensitisation of TPD (4M)-MEH-M3EH-PPV compared to TPD (4M)-MEH-PPV may be the lower average molar mass of the TPD (4M)-MEH-M3EH-PPV polymer than for TPD (4M)-MEH-PPV (35700 {29 repeated units} < 53100 g/mol {66 repeated units})[9]. Photoinduced charge transfer yield and recombination kinetics were also measured on ITO / HBL / Porous TiO_2 / polymer samples (without PEDOT and Au) using nanosecond–millisecond transient optical spectroscopy as described in Ref [4]. Such measurements of the photoinduced charge transfer yield confirm that infiltration of all of these polymers into the porous TiO_2 is excellent[17].

3.2.1 Effect of spectral absorbance

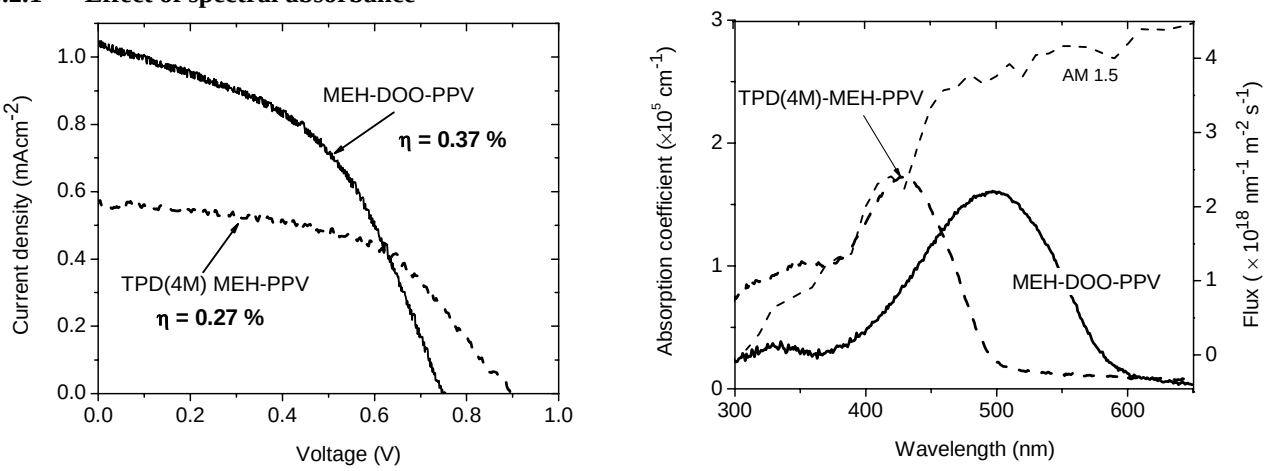

(a) (b)

Figure 6 (a) J-V characteristics of ITO / HBL (50 nm) / Porous TiO_2 (100 nm) / polymer (50 nm) / PEDOT/ Au devices under simulated (100 $mWcm^{-2}$, air mass 1.5) solar illumination. The polymers used were MEH-DOO-PPV and TPD-(4M)-MEH-PPV.(b) Optical absorption spectra of the two polymers compared with the AM 1.5 solar photon flux spectrum.

Figure 6 (a) shows the J-V characteristics of MEH-DOO-PPV and TPD (4M)-MEH-PPV polymer devices under simulated (100 $mWcm^{-2}$, air mass 1.5) solar illumination. The device structure was ITO / HBL (50 nm) / porous TiO_2 (100 nm) / polymer (50 nm) / PEDOT/ Au in both cases. The optical absorption spectra of these polymers are compared with the solar photon flux spectrum in Figure 6 (b). The MEH-DOO-PPV polymer device produced the higher short circuit current density, J_{SC}, of more than 1 $mAcm^{-2}$, while the TPD (4M)-MEH-PPV polymer showed the higher V_{OC} of 0.92 V and better overall device performance. The lower $J_{SC,}$ of 0.55 $mAcm^{-2}$ for TPD (4M)-MEH-PPV polymer compared to the MEH-DOO-PPV polymer can be attributed to the blue shifted absorption and lower spectral overlap with the solar photon flux spectrum. Nevertheless, the power conversion efficiency of this TPD (4M)-MEH-PPV device, at 0.27 %, is 50 % higher than the best previously reported efficiency for a hybrid TiO_2/polymer solar cell[6]. The low J_{SC} observed for the TPD (4M)-MEH-PPV polymer, with mobility more than two orders of magnitude greater than MEH-DOO-PPV polymer, indicates that in these devices, light harvesting properties play a more important role than charge transport in determining $J_{SC.}$ The larger V_{OC} for TPD (4M)-MEH-PPV than for MEH-DOO-PPV polymer devices may result from either the higher hole-mobility, the larger separation between the HOMO level of the polymer and the conduction band of TiO_2, or both. The influence of the hole-mobility on overall device performance will be discussed in section 3.2.3.

3.2.2 Importance of longer exciton diffusion length of polymer

Here we focus on device performance of F8T2 and TPD (4M) MEH-M3EH-PPV polymers in an optimised device structure consisting of ITO / HBL (50 nm) / porous TiO_2 (100 nm) / polymer (50 nm) / PEDOT/ Au. Figure 7 (a) shows J-V characteristics of F8T2 and TPD-(4M)-MEH-M3EH-PPV polymer devices under simulated (100 $mWcm^{-2}$, air mass 1.5) solar illumination. The device with F8T2 polymer shows power conversion efficiency of 0.21 %, while TPD-(4M)-MEH-M3EH-PPV polymer device shows 0.40 %. Although the device with F8T2 polymer shows better device performance than any previously reported TiO_2 / polymer solar cell[6], green photoluminescence from the device is still observed, when it is illuminated with a blue monochromatic light of wavelength 470 nm. This is probably due to the short exciton diffusion length of F8T2 polymer (see section 3.1.4). The SEM images of the porous film show that there are some large pores of more than 20 nm in the spin coated porous TiO_2 films. Figure 7 (b) illustrates how the exciton diffusion length of a polymer, compared to the pore size, may influences the charge separation. Since the exciton diffusion length of the F8T2 polymer is around a few nm, only excitons produced near to the interface contribute to the photocurrent and the rest of them recombine and emit luminescence. On the other hand, the longer exciton diffusion length of TPD (4M) MEH-M3EH-PPV polymer should enable more excitons to diffuse to the TiO_2 / polymer interface without recombining and then dissociate at the interface. A longer exciton diffusion length polymer is expected to reduce the losses by exciton recombination and offer higher photocurrent density.

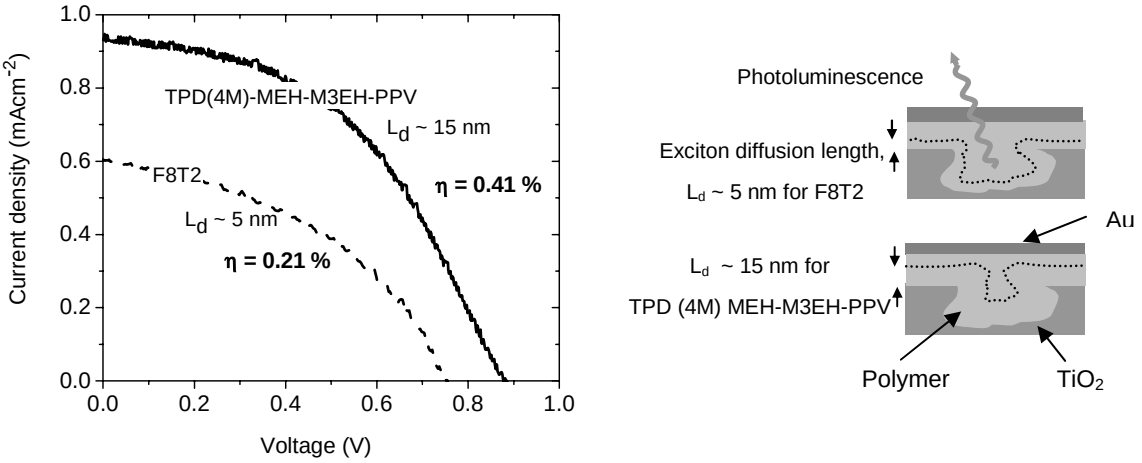

(a) (b)

Figure 7 (a) J-V characteristics of ITO / HBL (50 nm) / Porous TiO_2 (100 nm) / polymer (50 nm) / PEDOT/ Au devices under simulated (100 $mWcm^{-2}$, air mass 1.5) solar illumination. The polymers used were F8T2 and TPD-(4M)-MEH-M3EH-PPV polymer. The optoelectronic properties of these polymers are tabulated in the table I. (b) A schematic representation of the interface between TiO_2 pore and polymer, with different exciton diffusion lengths.

Although the F8T2 polymer has comparable hole-mobility and a higher absorption coefficient over a similar spectral range to the TPD (4M) MEH-M3EH-PPV polymer, F8T2 based polymer devices show a lower short circuit current density. This is probably due to the shorter exciton diffusion length of the F8T2 polymer (~5nm), stressing another key factor, apart from light harvesting, in photocurrent generation.

3.2.3 Influence of hole mobility of the polymer

Table II summarises the optoelectronic properties of the polymers studied and the performance of the corresponding devices. It has been reported[18] that open circuit voltage, V_{OC} in polymer / fullerene solar cells is strongly influenced by the energy separation between the HOMO level of the polymer and LUMO level of the fullerene, and the differences in workfunction of the electrodes influence the V_{OC} in a minor way. We may therefore expect better V_{OC} in F8T2 device than the TPD (4M) MEH-PPV device due to larger energy separation between the HOMO level of the polymer and the conduction band of TiO_2. However, TPD (4M)-MEH-PPV polymer device offers the larger V_{OC} than high I_P F8T2 polymer devices. This may result from the higher hole-mobility of TPD (4M)-MEH-PPV polymer which may minimise interfacial recombination. The table further shows that the fill factor the device also appears to be weakly correlated to the hole-mobility of the polymer. Higher hole-mobility polymer devices offer better fill factor and V_{OC}. The influence of the hole-mobility on overall device performance cannot, therefore, be ruled out.

Table II The influence of optoelectronic properties of polymers on photovoltaic parameters of the devices

Polymers	**TPD (4M)-MEH-PPV**	**MEH-DOO-PPV**	**TPD (4M)-MEH-M3EH-PPV**	**F8T2**
λmax (nm)	425	502	440	460
I_P (eV)	5.45	5.25	5.30	5.55
μ_h (cm^2/Vs)*	**10^{-3}**	**10^{-5}**	10^{-4}	10^{-5}- 10^{-4}
L (nm)	~ 15	~ 15	**~ 15**	**~ 5**
J_{SC} ($mAcm^{-2}$)	0.57	1.04	**0.96**	**0.60**
V_{OC}	**0.90**	**0.74**	0.86	0.75
FF	0.53	0.48	0.50	0.46
η (%)	**0.27**	**0.37**	**0.41**	**0.21**

* at 2.5×10^5 V/cm

In summary, the device made from TPD (4M)-MEH-M3EH-PPV polymer showed the best performance. This is due to the best combination of properties for the TPD (4M)-MEH-M3EH-PPV polymer, such as high hole-mobility, good visible absorption, long exciton diffusion length (~15 nm) and moderate ionisation potential (5.30 eV) as well as its ability to sensitise TiO_2 (possibly assisted by the alkoxy side chain oxygen atoms). The fluorene thiophene copolymer device shows poorer performance than the MEH-PPV based polymer devices, despite having similar or better light absorption and charge transport properties. This is probably due to the shorter exciton diffusion length for this polymer.

3.3 Optimising device performance

3.3.1 Improvement of hole collection using PEDOT

Here, we report the effect of PEDOT on charge collection. Figure 8 (a) shows J-V characteristics in dark and under AM1.5 equivalent illumination (100mWcm^{-2}), of F8T2 devices with and without the PEDOT layer. The PEDOT layer increases the J_{SC} from 0.4 mAcm^{-2} to 0.6 mAcm^{-2}. The V_{OC}, however, decreases by about 0.2 V. The overall efficiency is increased from 0.17 % to 0.21 %. Similar observations were also found in TPD (4M)-MEH-M3EH-PPV and the other MEH-PPV polymer devices[17,19].

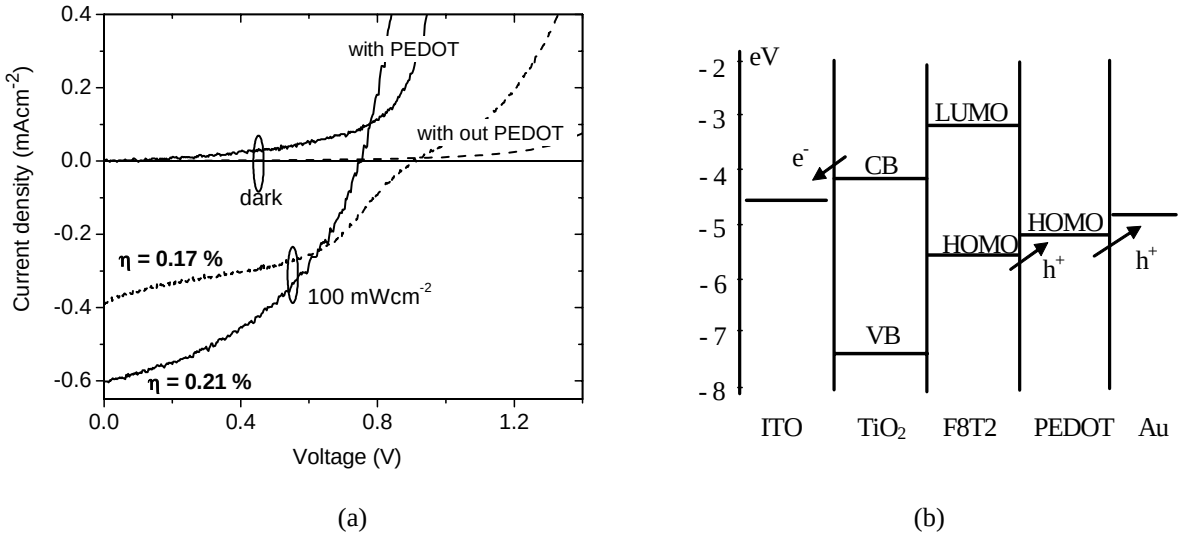

(a) (b)

Figure 8 (a) J–V characteristics in dark and under AM 1.5 solar spectrum irradiation (100 mW cm^{-2}, 1 sun), of F8T2 devices (ITO / HBL / Porous TiO_2 (100 nm) / F8T2 (50 nm) / PEDOT/ Au) with (solid lines) or without the PEDOT layer (dash lines) and (b) the corresponding energy band diagram for this multilayer device.

There are several possible reasons for the improvement in J_{SC} resulting from insertion of the PEDOT layer. One explanation is that PEDOT may cause a chemical doping of the polymer that reduces the contact resistance between the polymer and metal contact. A second possibility is that the PEDOT layer may protect the polymer film from damage during evaporation of the Au electrode[20], which could lead to an increase in the series resistance of the device. A third possibility is that PEDOT improves collection by minimising the energy step between polymer and top contact (see Figure 8 (b)). Experimental[4] and simulation[21] studies show that interfacial energy steps should be minimised for efficient charge transfer between active layers and electrodes. It has also been shown that the workfunction of Au on top of conjugated polymers may be smaller than the expected value of 5.1 eV by 0.2-0.3 eV[22]. Since the ionisation potential of F8T2 polymer is 5.55 eV, the energy step at the polymer/Au interface is expected to be at least 0.6 eV in the device without the PEDOT layer. In contrast, for the device with the PEDOT layer, the interfacial energy step should be reduced because the PEDOT workfunction is about 5.3 eV. The dark J-V shows that the forward-bias dark current for the device with PEDOT is much higher (110 times at + 1.0 V) than for the device without PEDOT, confirming that the energy barrier for hole injection at the polymer / metal interface is reduced by introduction of the PEDOT layer. The decrease in V_{OC} upon introduction of the PEDOT layer is also quite consistent with a reduced interfacial energy step and increased hole-injection. Note that the effect on V_{OC} is the reverse of that expected, if V_{OC} were controlled by the difference in electrode workfunctions. Although the exact mechanism by which PEDOT increases J_{SC} is not clear, it appears to be related to the improved conductivity of the polymer / top contact interface.

3.3.2 Effect of active layer thickness

In this study, the organic paste was used to study the effect of the thickness of the porous layers on devices performance. The TPD (4M)-MEH-M3EH-PPV polymer was chosen as hole transporting materials to optimise the device performance. The inset to Figure 9 (a) shows the AM 1.5 power conversion efficiencies for devices with different porous TiO_2 layer thicknesses, from 100 nm to 500 nm for a fixed polymer thickness of 100 nm. The efficiency is maximum when the ratio of the porous TiO_2 layer thickness to the effective polymer layer thickness is about 2:1. This result is reasonable, since there should be exactly enough polymer to fill the pores at this ratio, assuming that the porosity of the TiO_2 films is 50 %[23]. Next, keeping the optimum ratio of 2:1 for the porous TiO_2 and polymer layer thicknesses the effect of total device thickness was studied. Figure 9 (a) compares the J-V characteristics for thick (200 nm porous TiO_2, 100 nm polymer) and thin (100 nm porous TiO_2, 50 nm polymer) devices under AM 1.5 conditions. The thin device shows an open circuit voltage V_{OC} = 0.64 V, a short circuit current density J_{SC} = 2.1 mA cm^{-2} and a fill factor of 0.43. Its resulting AM 1.5 power conversion efficiency, 0.58 %, is more than twice that of the thick device, namely 0.27 %. The higher efficiency may be attributed to a reduced series resistance for the thinner TiO_2 and polymer layers, and to improved charge collection efficiency. Figure 9 (b) shows the external quantum efficiency spectrum of the thin device together with the absorption spectrum of the semiconducting polymer. The device shows a maximum external quantum efficiency of 40 % at the maximum absorption of the polymer. Integrating the product of the measured EQE with the photon flux density of the AM1.5 solar spectrum yields a maximum short circuit current density of about 2.5 $mAcm^{-2}$, which is consistent with the measured J_{SC} under AM1.5 conditions of 2.1 mA cm^{-2}.

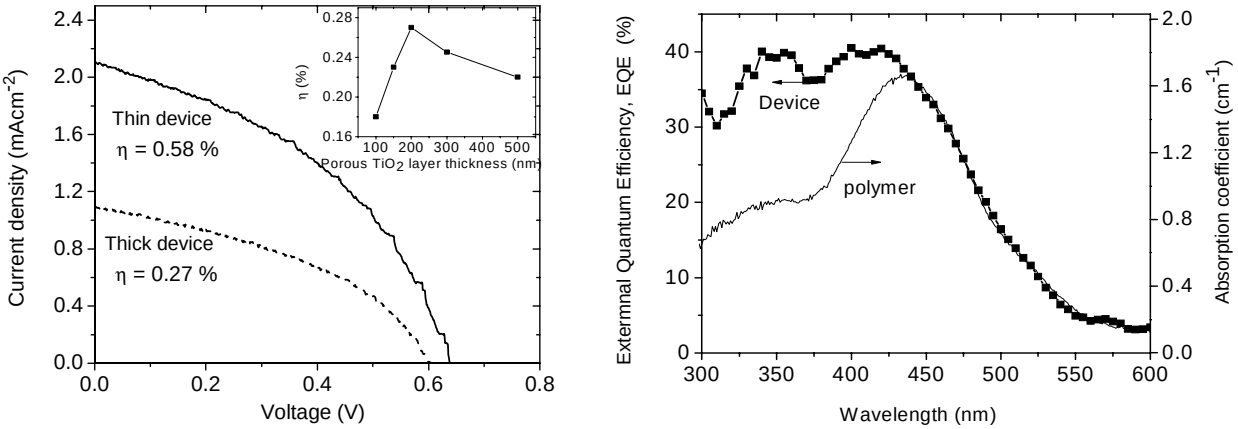

(a) (b)

Figure 9 (a) J-V characteristics (under A.M. 1.5 conditions (1 sun)) for both thick (200 nm porous TiO_2, 100 nm polymer) and thin (100 nm porous TiO_2, 50 nm polymer) multilayer devices. The inset shows the AM 1.5 power conversion efficiency for devices with different porous layer thicknesses for a constant polymer thickness (100nm) and (b) quantum efficiency spectrum of the thin multilayer device (filled squares) and the corresponding absorption spectrum of the polymer (solid line).

4. CONCLUSIONS

We study the relationship between polymer optoelectronic properties and the performance of polymer / TiO_2 hybrid photovoltaic devices. We conclude that the polymer properties with greatest influence on device efficiency are the polymer exciton diffusion length and absorption range, followed by the hole-mobility. We find strong effect both from introduction of a PEDOT layer and from optimising the active layer thickness. We report multilayer hybrid TiO_2 / polymer photovoltaic devices based on nanocrystalline TiO_2 and a TPD containing MEH-PPV polymer, with the highest power conversion efficiency to date.

ACKNOWLEDGEMENTS

We are grateful to The Dow Chemical Company and Prof. H. H. Horhold for providing the polymer samples and to Dr. J. M. Kroon for supplying their TiO_2 paste. P. Ravirajan acknowledges the Association of Commonwealth Universities for a Commonwealth Scholarship and J. Nelson and J. R. Durrant acknowledge the EPSRC for financial support.

REFERENCES

1 P. Schilinsky, C. Waldauf, and C. J. Brabec, "Printed plastic solar cells with power conversion efficiency of 5 %", SCELL-2004, Badajoz, Spain; F. Padinger, R. S. Rittberger, and N. S. Sariciftci, "Effects of postproduction treatment on plastic solar cells", Adv. Funct. Mater. **13** (1), 85-88 (2003); C. J. Brabec, S. E. Shaheen, C. Winder, N. S. Sariciftci, and P. Denk, "Effect of LiF/metal electrodes on the performance of plastic solar cells", Appl. Phys. Lett. **80** (7), 1288-1290 (2002).

2 T. J. Savenije, J. M. Warman, and A. Goossens, "Visible light sensitisation of titanium dioxide using a phenylene vinylene polymer," Chem. Phys. Lett. **287** (1-2), 148-153 (1998).

3 K. M. Coakley and M. D. McGehee, "Photovoltaic cells made from conjugated polymers infiltrated into mesoporous titania," Appl. Phys. Lett. **83** (16), 3380-3382 (2003); P. A. van Hal, M. M. Wienk, J. M. Kroon, W. J. H. Verhees, L. H. Slooff, W. J. H. van Gennip, P. Jonkheijm, and R. A. J. Janssen, "Photoinduced electron transfer and photovoltaic response of a MDMO-PPV : TiO_2 bulk-heterojunction", Adv. Mater. **15** (2), 118-121 (2003).

4 P. Ravirajan, S. A. Haque, J. R. Durrant, D. Poplavskyy, D. D. C. Bradley, and J. Nelson, "Hybrid nanocrystalline TiO2 solar cells with a fluorene- thiophene copolymer as a sensitizer and hole conductor", J. Appl. Phys. **95** (3), 1473-1480 (2004).

5 A. C. Arango, L. R. Johnson, V. N. Bliznyuk, Z. Schlesinger, S. A. Carter, and H. H. Horhold, "Efficient titanium oxide/conjugated polymer photovoltaics for solar energy conversion", Adv. Mater. **12** (22), 1689-1692 (2000).

6 A. J. Breeze, Z. Schlesinger, S. A. Carter, and P. J. Brock, "Charge transport in TiO2/MEH-PPV polymer photovoltaics", Phys. Rev. B **6412** (12), 125205 (2001).

7 J. Nelson, M. Eppler, D. Poplavskyy, P. Ravirajan, D.C.C. Bradley, J.R. Durrant, and S. A. Haque, "Conjugated fluorene copolymers as hole transport materials in polymer-metal oxide photovoltaic devices", Proc. 201st Meeting of The Electrochemical Society, (2002).

8 S. Pfeiffer and H. H. Horhold, "Synthesis of soluble MEH-PPV and MEH-PPB by HORNER condensation polymerization", Synth. Met. **101** (1-3), 109-110 (1999); H. H. Horhold, H. Tillmann, C. Bader, R. Stockmann, J. Nowotny, E. Klemm, W. Holzer, and A. Penzkofer, "MEH-PPV and dialkoxy phenylene vinylene copolymers. Synthesis and lasing characterization", Synth. Met. **119** (1-3), 199-200 (2001).

9 W. Holzer, A. Penzkofer, H. Tillmann, D. Raabe, and H. H. Horhold, "Photo-physical characterisation and travelling-wave lasing of some TPD-based polymer neat films", Opt. Mater. **19** (2), 283-294 (2002).

10 R. L. Willis, C. Olson, B. O'Regan, T. Lutz, J. Nelson, and J. R. Durrant, "Electron dynamics in nanocrystalline ZnO and TiO2 films probed by potential step chronoamperometry and transient absorption spectroscopy", J. Phys. Chem. B **106** (31), 7605-7613 (2002).

11 M. Spath, P. M. Sommeling, J. A. M. van Roosmalen, H. J. P. Smit, N. P. G. van der Burg, D. R. Mahieu, N. J. Bakker, and J. M. Kroon, "Reproducible manufacturing of dye-sensitized solar cells on a semi-automated baseline", Prog. Photovoltaics **11** (3), 207-220 (2003).

12 P. Ravirajan, S. A. Haque, D. Poplavskyy, J. R. Durrant, D. D. C. Bradley, and J. Nelson, "Solid state solar cell made from nanocrystalline TiO2 with a fluorene-thiophene copolymer as a hole conductor", Proc. SPIE Int. Soc. Opt. Eng. **5215**, 226-236 (2004).

13 L. Kavan and M. Gratzel, "Highly Efficient Semiconducting Tio2 Photoelectrodes Prepared by Aerosol Pyrolysis", Electrochim. Acta **40** (5), 643-652 (1995).

14 J. Huang, P. F. Miller, J. C. de Mello, A. J. de Mello, and D. D. C. Bradley, "Influence of thermal treatment on the conductivity and morphology of PEDOT/PSS films", Synth. Met. **139** (3), 569-572 (2003).

15 R. Rawcliffe (Private communication).

16 H. Sirringhaus, R. J. Wilson, R. H. Friend, M. Inbasekaran, W. Wu, E. P. Woo, M. Grell, and D. D. C. Bradley, "Mobility enhancement in conjugated polymer field-effect transistors through chain alignment in a liquid-crystalline phase", Appl. Phys. Lett. **77** (3), 406-408 (2000).

17 P. Ravirajan, S. A. Haque, J. R. Durrant, D. D. C. Bradley, and J. Nelson, ""The effect of polymer optoelectronic properties on the performance of multilayer hybrid polymer/TiO2 solar cells", Adv. Funct. Mater. (submitted).

18 C. J. Brabec, A. Cravino, D. Meissner, N. S. Sariciftci, T. Fromherz, M. T. Rispens, L. Sanchez, and J. C. Hummelen, "Origin of the open circuit voltage of plastic solar cells," Adv. Funct. Mater. **11** (5), 374-380 (2001).

19 P. Ravirajan, S. A. Haque, J. R. Durrant, H. J. P. Smit, J. M. Kroon, D. D. C. Bradley, and J. Nelson, Appl. Phys. Lett. (submitted).

20 A. Ioannidis, J. S. Facci, and M. A. Abkowitz, "Evolution in the charge injection efficiency of evaporated Au contacts on a molecularly doped polymer", J. Appl. Phys. **84** (3), 1439-1444 (1998).

21 J. Nelson, J. Kirkpatrick, and P. Ravirajan, "Factors limiting the efficiency of molecular photovoltaic devices", Phys. Rev. B **69** (3), 035337 (2004).

22 G. G. Malliaras, J. R. Salem, P. J. Brock, and C. Scott, "Electrical characteristics and efficiency of single-layer organic light-emitting diodes", Phys. Rev. B **58** (20), R13411-R13414 (1998); A. J. Campbell, D. D. C. Bradley, and H. Antoniadis, "Quantifying the efficiency of electrodes for positive carrier injection into poly(9,9-dioctylfluorene) and representative copolymers", J. Appl. Phys. **89** (6), 3343-3351 (2001).

23 C. J. Barbe, F. Arendse, P. Comte, M. Jirousek, F. Lenzmann, V. Shklover, and M. Gratzel, "Nanocrystalline titanium oxide electrodes for photovoltaic applications", J. Am. Ceram. Soc. **80** (12), 3157-3171 (1997).